SMC-TR-94-27

AEROSPACE REPORT NO.
TR-93(3925)-4

Improved Performance of Degraded Solar Arrays at Non-Zero Sun Incidence Angles

15 May 1993

Prepared by

D. C. MARVIN
Electronics Technology Center
Technology Operations

Prepared for

SPACE AND MISSILE SYSTEMS CENTER
AIR FORCE MATERIEL COMMAND
2430 E. El Segundo Boulevard
Los Angeles Air Force Base, CA 90245

Development Group

THE AEROSPACE CORPORATION
El Segundo, California

This report was submitted by The Aerospace Corporation, El Segundo, CA 90245-4691, under Contract No. F04701-88-C-0089 with the Space and Missile Systems Center, 2430 E. El Segundo Blvd., Los Angeles Air Force Base, CA 90245. It was reviewed and approved for The Aerospace Corporation by S. Feuerstein, Acting Principal Director, Electronics Technology Center. Capt. Louis Poehlman was the project officer.

This report has been reviewed by the Public Affairs Office (PAS) and is releasable to the National Technical Information Service (NTIS). At NTIS, it will be available to the general public, including foreign nationals.

This technical report has been reviewed and is approved for publication. Publication of this report does not constitute Air Force approval of the report's findings or conclusions. It is published only for the exchange and stimulation of ideas.

Louis Poehlman, Capt. USAF
SMC/IMO

UNCLASSIFIED

SECURITY CLASSIFICATION OF THIS PAGE

REPORT DOCUMENTATION PAGE

1a. REPORT SECURITY CLASSIFICATION Unclassified	1b. RESTRICTIVE MARKINGS
2a. SECURITY CLASSIFICATION AUTHORITY	3. DISTRIBUTION/AVAILABILITY OF REPORT Approved for public release; distribution unlimited
2b. DECLASSIFICATION/DOWNGRADING SCHEDULE	
4. PERFORMING ORGANIZATION REPORT NUMBER(S) TR-93(3925)-4	5. MONITORING ORGANIZATION REPORT NUMBER(S) SMC-TR-94-27
6a. NAME OF PERFORMING ORGANIZATION The Aerospace Corporation Technology Operations 6b. OFFICE SYMBOL *(If applicable)*	7a. NAME OF MONITORING ORGANIZATION Space and Missile Systems Center
6c. ADDRESS *(City, State, and ZIP Code)* El Segundo, CA 90245-4691	7b. ADDRESS *(City, State, and ZIP Code)* Los Angeles Air Force Base Los Angeles, CA 90009-2960
8a. NAME OF FUNDING/SPONSORING ORGANIZATION 8b. OFFICE SYMBOL *(If applicable)*	9. PROCUREMENT INSTRUMENT IDENTIFICATION NUMBER F04701-88-C-0089
8c. ADDRESS *(City, State, and ZIP Code)*	10. SOURCE OF FUNDING NUMBERS PROGRAM ELEMENT NO. / PROJECT NO. / TASK NO. / WORK UNIT ACCESSION NO.

11. TITLE *(Include Security Classification)*

Improved Performance of Degraded Solar Arrays at Non-Zero Sun Incidence Angles

12. PERSONAL AUTHOR(S)
Marvin, Dean C.

13a. TYPE OF REPORT	13b. TIME COVERED FROM _____ TO _____	14. DATE OF REPORT *(Year, Month, Day)*	15. PAGE COUNT
		15 May 1993	17

16. SUPPLEMENTARY NOTATION

17. COSATI CODES			18. SUBJECT TERMS *(Continue on reverse if necessary and identify by block number)*
FIELD	GROUP	SUB-GROUP	Solar-Array Degradation, Solar-Array Temperature, Solar-Array Pointing

19. ABSTRACT *(Continue on reverse if necessary and identify by block number)*

A silicon solar array was flown in a high-radiation orbit with thin cover glasses. As a result, severe radiation degradation occurred. It was discovered that as degradation proceeded, the maximum array output current was obtained for sun incidence angles other than 0° for some bus voltages. Optimum angles as high as 38° have been observed. The analysis reported herein was undertaken in order to quantitatively explain the observed sun angle and bus voltage dependence of the array current. The resulting model, which includes temperature and radiation effects on the solar cell properties, was able to account for all of the flight data that have been collected, and can be used for power management planning purposes on this vehicle.

20. DISTRIBUTION/AVAILABILITY OF ABSTRACT	21. ABSTRACT SECURITY CLASSIFICATION
[X] UNCLASSIFIED/UNLIMITED [ ] SAME AS RPT. [ ] DTIC USERS	Unclassified

22a. NAME OF RESPONSIBLE INDIVIDUAL	22b. TELEPHONE *(Include Area Code)*	22c. OFFICE SYMBOL

DD FORM 1473, 84 MAR

83 APR edition may be used until exhausted.
All other editions are obsolete.

SECURITY CLASSIFICATION OF THIS PAGE
UNCLASSIFIED

CONTENTS

FIGURES

TABLES

1. INTRODUCTION

The end-of-life operation of spacecraft is often characterized by the need for careful electrical power management. This requires accurate knowledge of payload electrical requirements, eclipse occurrence and duration, battery conditions, and solar-array output capability. Typically, the solar-array output has degraded in a steady, well-understood manner determined by the array components and the radiation properties of the orbit. This study was undertaken near the end of life of a vehicle when such power management methods were in use. The unusual aspect of this system was the observation that the solar array produced more output current when pointed somewhat away from the sun. The deviation from zero sun angle that produced the maximum output was empirically found to depend on the exact bus voltage set point and the age of the array. Since the array was continuing to age, and accurate output current predictions were needed, a study was commissioned to model the array behavior.

2. MODEL DETAILS

The principal aspects of the solar-array model are the solar cell beginning-of-life (BOL) and end-of-life (EOL) electrical parameters, and the steady-state temperature of the array. The important electrical parameters are the short-circuit current, I_{sc}, the open circuit voltage, V_{oc}, and the current, I_{mp}, and voltage, V_{mp}, at the maximum point. The temperature coefficients of these parameters and the effect of radiation on the parameters are critical as well.

2.1 ARRAY TEMPERATURE

The temperature of a solar array can be generally described by the function

$$T = \left[\frac{(\alpha - \eta) q \cos\theta + q'}{\varepsilon \sigma} \right]^{\frac{1}{4}}, \tag{1}$$

where α is the solar cell absorptivity, η is the cell efficiency, q is the solar intensity, θ is the sun angle, q' accounts for the earth's albedo, ε is the total array emissivity, and σ is the Stefan-Boltzmann constant. In order to compute the temperature directly, each of these terms must be known. For the present problem, temperature telemetry data were available from sensors located on the backside of the array. These data were used to simplify Eq. (1) to

$$T = T_0 \left[\frac{1 + K \cos\theta}{1 + K} \right]^{\frac{1}{4}}, \tag{2}$$

where K is a constant, and T_0 is the temperature at zero sun angle. Figure 1 shows the quality of fit to the flight data that this functional form provides. This agreement was judged to be adequate for the problem. Ground test results and a detailed thermal model had shown previously that a 10°C differential exists between the front and back of the panel under a wide range of steady-state and transient conditions. Therefore, the function in Eq. (2) was used to predict the backside temperature, and the frontside temperature representing the solar cells was assumed to be 10°C above this.

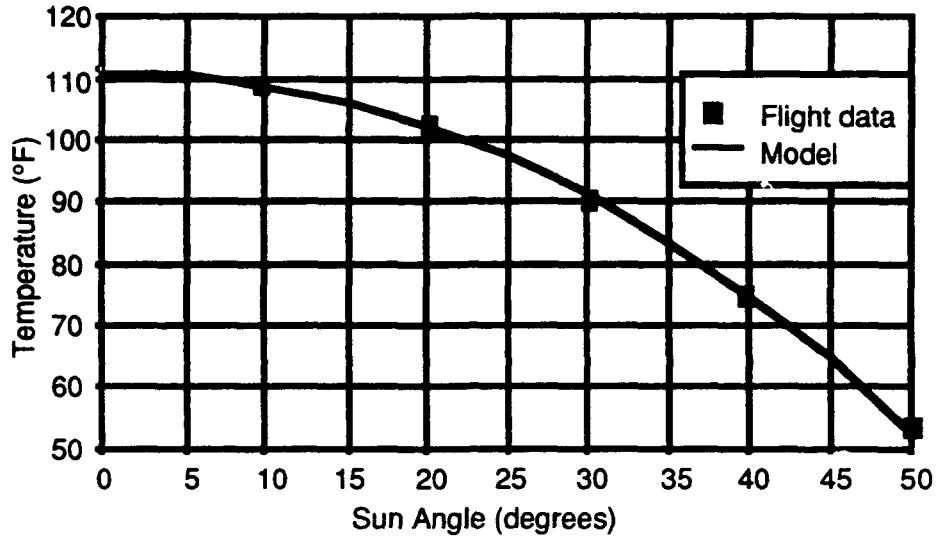

Figure 1. Array temperature from flight data (symbols) and model (line).

2.2 FORM OF ARRAY IV CURVE

The array current-voltage behavior (IV curve) was assumed to be related to the individual solar cell IV curves by the following,

$$V_{array} = V_{cell} * N_{series} - V_{diode} - V_{iR} \quad (3)$$

$$I_{array} = I_{cell} * (N_{parallel} - N_{fail}) * I_{sun} * F * \cos\theta\ , \quad (4)$$

where the N_i refer to the number of cells in series, in parallel, or failed open, as labeled; I_{sun} is the relative solar intensity; and F is a factor that includes miscellaneous losses such as cell matching at assembly, adhesive darkening, etc.

The IV curve of a solar cell was modeled by the expression (Ref. 1)

$$I(V) = (I_{sc} - B*(\exp((V_{cell}/C) - 1)), \quad (5)$$

where

$$V_{array} = V_{cell} + V_{diode} + V_{iR} \quad (6)$$

$$C = (V_{mp} - V_{oc})/\ln(1 - I_{mp}/I_{sc}) \quad (7)$$

$$B = (I_{sc} - I_{mp})*\exp(-V_{mp}/C). \quad (8)$$

The advantage of this expression is that it only requires knowledge of the three prime points (I_{sc}, V_{oc}, P_{max}) of the cell in order to generate the complete IV curve. It has been found to accurately represent the behavior of Si solar cells at both beginning of life and after significant radiation degradation, and over an appropriate range of operating temperatures.

2.3 SOLAR CELL PRIME POINTS

In order to reproduce the array effects observed in the flight data, it is essential to have accurate knowledge of the solar-cell prime points as a function of temperature and radiation dose. The temperature dependence is customarily expressed in terms of temperature coefficients, which may vary in different temperature ranges. For a constant temperature coefficient k, the equation describing the variation of a parameter is simply

$$X(T) = X(28^\circ\ C)*k*(T - 28^\circ\ C)\ , \quad (9)$$

where X is the prime point variable. The radiation degradation is based primarily on empirical data and typically takes the form

$$X/X_0 = 1\text{-}A*\ln(1+\phi/\phi_0)\ , \quad (10)$$

where A and ϕ_0 are parameters, X_0 is the beginning-of-life value and ϕ is the actual equivalent 1 MeV electron fluence.

This rather simple view of these effects is complicated by the second-order effect of temperature coefficient variation with radiation. However, it is found that at the high radiation doses this array has experienced (on the order of 6E15 equivalent 1 MeV electrons/cm^2), the temperature coefficients have essentially reached asymptotic with respect to radiation effects.

The values of the parameters in Eqs. (9) and (10) are obtained from qualification tests performed on the solar cells prior to their use. For the K6 3/4 silicon solar cells used on the subject array, there were two qualification test documents available. These are referred to as the Preflight Test and the Hughes Miniqual Test (Ref. 2). Table 1 compares these parameters.

Given the differences in these values and some questionable temperature behavior of the Preflight Test data, the Miniqual data were selected for use. A 10% uncertainty was assigned to all of the temperature coefficients.

Table 1. Comparison of K6 3/4 Solar Cell Parameters from Two Qualification Tests

Parameter	Preflight	Mini-qual
Temp. Coeff.		
I_{sc} (A/cm^2)	6.50E-05	5.90E-05
V_{oc} (V)	-2.13E-03	-2.25E-03
I_{mp} (A/cm^2)	2.70E-05	4.20E-05
V_{mp} (V)	-2.41E-03	-2.22E-03
Radiation		
I_{sc}		
A	0.0593	0.0543
ϕ_0	5.25E+13	3.41E+13
V_{oc}		
A	0.0312	0.0272
ϕ_0	1.20E+13	1.15E+13
I_{mp}		
A	0.107	0.0582
ϕ_0	2.54E+14	4.18E+13
V_{mp}		
A	0.0306	0.0258
ϕ_0	9.63E+12	7.79E+12

3. FLIGHT DATA

The flight data shown in Table 2 were provided for validation of the model. The output current of the +Y solar array wing was measured as a function of solar incidence angle and bus voltage. The data were taken in rapid succession to minimize changes in sun angle and albedo. The range specified for each angle/voltage combination is the 95% confidence interval based on multiple measurements. The uncertainty in the bus voltage values is 150 mV.

Table 2. Current (amps) from +Y array wing.

Bus voltage	30.13 V	30.53 V	31.06 V	31.53 V
Angle				
15	19.78-19.86	19.30-19.40	18.51-18.59	17.76-18.06
18	19.79-19.89	19.37-19.45	18.57-18.69	17.98-18.11
23	19.73-19.83	19.26-19.43	18.63-18.95	17.96-18.14
27	19.56-19.76	19.27-19.39	18.73-18.81	18.19-18.41
35		18.93-19.03	18.48-18.64	18.07-18.21

4. ANALYSIS

At the time the flight data were taken, the equivalent 1 MeV electron fluence received by the solar array was 6.24E15 cm^{-2} for I_{sc} and 1.35E16 cm^{-2} for V_{oc}, I_{mp}, and V_{mp}. Figure 2 shows the IV curve for the array at BOL (dashed curves) and at present (solid curves) for two temperatures. These temperatures, 43°C and 54°C, are the frontside array temperatures at solar incidence angles of 0° and 30°, respectively.

The parameters in Table 1 are not listed explicitly in the qualification test documents. Rather, they have been obtained by fitting curves to graphical representations of the data in the documents. The temperature coefficients in the table are valid only in the range $0 < T < 60°C$ and for radiation doses (equivalent 1 MeV electron fluence) > 1E15 cm^{-2}. Both of these constraints are satisfied in the present problem. The radiation degradation parameters A and ϕ_0 are obtained by fitting Eq. (9) to the data.

The observed angle dependence of the array output can be understood qualitatively as follows. The power system is shunt regulated and designed to operate at approximately 30 to 33 V. This voltage range operates the solar cells to the left of P_{max}. Figure 2 shows no significant temperature dependence of output current in this region at BOL. However, at the high radiation doses experienced, these operating voltages lie near or to the right of P_{max}. The output current of the degraded array is then very sensitive to temperature because of the proximity of the operating voltages to V_{oc}. Figure 2 illustrates the large variation in current that can be caused by a tempera-

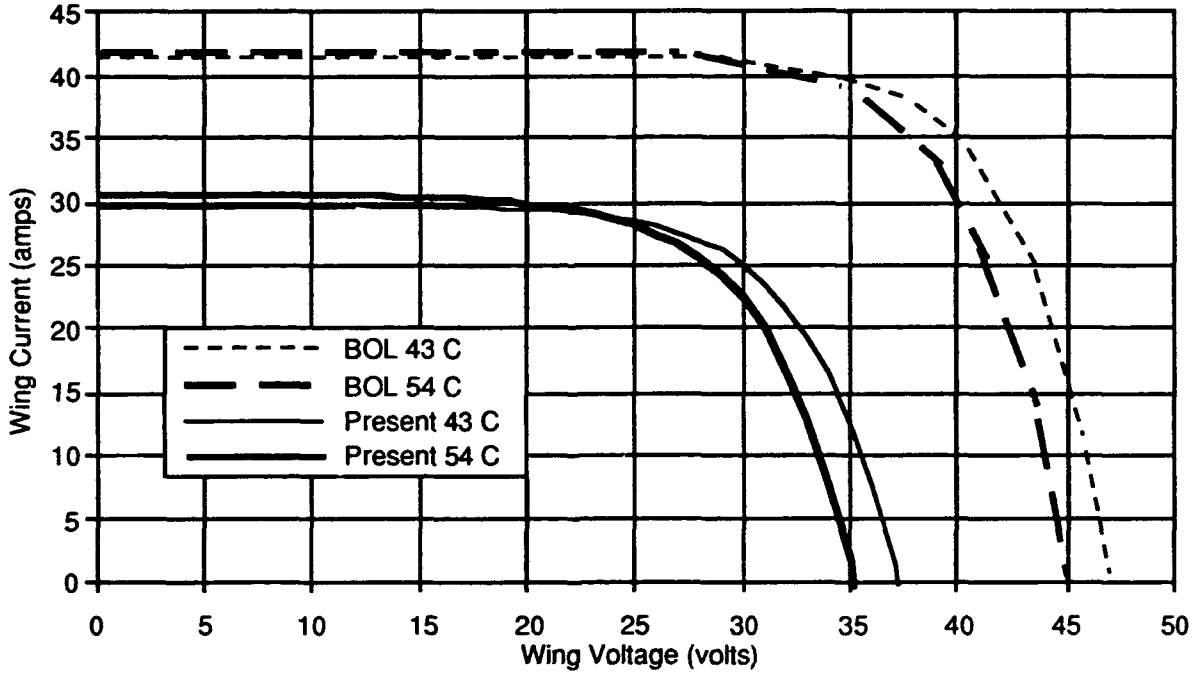

Figure 2. Broken lines show current-voltage behavior for array at two temperatures at beginning of life. Solid lines are for present state of degradation.

ture change under these operating conditions. Therefore, under some conditions, it might be expected that when the array is pointed off from the sun vector, the gain in current resulting from the lower array temperature might overcome the cosine factor loss in current.

Figure 3 shows the flight data in Table 2 (symbols) and the predictions of the model detailed above (curves). Two symbols are used for each data point, representing the upper and lower 95% confidence limits shown in the table. All of the data were measured in the same week in 1992 with the exception of the 32.6-V data set, which was taken in 1991. The agreement between the model and the data is quite good in two important respects. First, the sun angle that produces the maximum current output is correct for all three bus voltages. Second, the magnitude of the maximum is well predicted. These are the two most important parameters used in determining the maximum array output capability and how to obtain it. Given this information, a low-risk power management plan can be implemented for use in eclipse season.

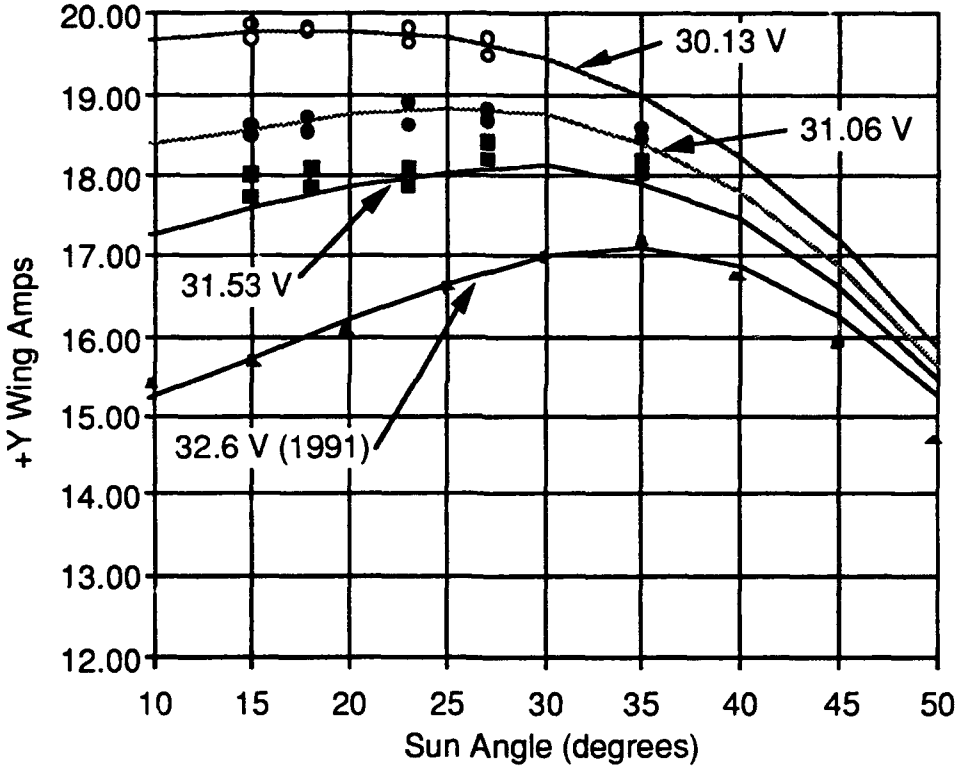

Figure 3. Model predictions (curves) and flight data (symbols) for off-pointed array performance as a function of sun angle. Double symbols are used to indicate 95% confidence limits of flight data.

5. SUMMARY

It has been observed that a solar array that has suffered significant radiation degradation produces maximum current output at non-zero sun incidence angles. An analysis has been presented that shows that this effect can be accurately modeled using radiation degradation and temperature coefficients. The net gain in current can be as great as 25% under realistic operating conditions. Furthermore, knowledge of the array performance characteristics enables a low-risk power management plan to be formulated for use during eclipse season.

REFERENCES

1. H.S. Rauschenbach 1980, Solar Cell Array Design Handbook, Van Nostrand Reinhold Co., New York.

2. L.J. Goldhammer 1979, K6 3/4 Solar Cell Miniqualification Program, Hughes Space and Communications Group, SCG 90259R.

TECHNOLOGY OPERATIONS

The Aerospace Corporation functions as an "architect-engineer" for national security programs, specializing in advanced military space systems. The Corporation's Technology Operations supports the effective and timely development and operation of national security systems through scientific research and the application of advanced technology. Vital to the success of the Corporation is the technical staff's wide-ranging expertise and its ability to stay abreast of new technological developments and program support issues associated with rapidly evolving space systems. Contributing capabilities are provided by these individual Technology Centers:

Electronics Technology Center: Microelectronics, solid-state device physics, VLSI reliability, compound semiconductors, radiation hardening, data storage technologies, infrared detector devices and testing; electro-optics, quantum electronics, solid-state lasers, optical propagation and communications; cw and pulsed chemical laser development, optical resonators, beam control, atmospheric propagation, and laser effects and countermeasures; atomic frequency standards, applied laser spectroscopy, laser chemistry, laser optoelectronics, phase conjugation and coherent imaging, solar cell physics, battery electrochemistry, battery testing and evaluation.

Mechanics and Materials Technology Center: Evaluation and characterization of new materials: metals, alloys, ceramics, polymers and their composites, and new forms of carbon; development and analysis of thin films and deposition techniques; nondestructive evaluation, component failure analysis and reliability; fracture mechanics and stress corrosion; development and evaluation of hardened components; analysis and evaluation of materials at cryogenic and elevated temperatures; launch vehicle and reentry fluid mechanics, heat transfer and flight dynamics; chemical and electric propulsion; spacecraft structural mechanics, spacecraft survivability and vulnerability assessment; contamination, thermal and structural control; high temperature thermomechanics, gas kinetics and radiation; lubrication and surface phenomena.

Space and Environment Technology Center: Magnetospheric, auroral and cosmic ray physics, wave-particle interactions, magnetospheric plasma waves; atmospheric and ionospheric physics, density and composition of the upper atmosphere, remote sensing using atmospheric radiation; solar physics, infrared astronomy, infrared signature analysis; effects of solar activity, magnetic storms and nuclear explosions on the earth's atmosphere, ionosphere and magnetosphere; effects of electromagnetic and particulate radiations on space systems; space instrumentation; propellant chemistry, chemical dynamics, environmental chemistry, trace detection; atmospheric chemical reactions, atmospheric optics, light scattering, state-specific chemical reactions and radiative signatures of missile plumes, and sensor out-of-field-of-view rejection.